**BOUNDARY CONDITIONS FOR THE FORMATION OF RAMPARTS ON FLUIDIZED EJECTA DEPOSITS AROUND MARTIAN IMPACT CRATERS.** S. A. Fagents[1], S. M. Baloga[2] and P. J. Mouginis-Mark[1], [1]HIGP/SOEST, University of Hawaii, 2525 Correa Road, Honolulu, HI 96822; fagents@hawaii.edu, [2]Proxemy Research 20528 Farcroft Lane, Laytonsville, MD 20882.

**Introduction:** Images from the MOC and THEMIS instruments are revealing in unprecedented detail the structure of fluidized ejecta deposits associated with certain martian impact craters. The two most common types have been formally classified by *Barlow et al*. [1] as single layered ejecta (SLE) and double layered ejecta (DLE) craters, although numerous examples of additional, highly complex, types of fluidized ejecta have now been documented [2]. The formation of the lobate deposits has been attributed to the presence of volatiles (water or ice) within the target material at the time of crater formation [3-7], or to atmospheric effects [8-9]. As such, fluidized ejecta provide a unique diagnostic of target properties and the ambient conditions at the time of impact. The spatial and temporal variations in ejecta characteristics can then be ascribed to target variations (e.g., volatile content), the latitude and elevation of the parent crater, and possible temporal changes in the climate [10-12].

We have developed a model of ejecta emplacement based on the assumption of continuum overland flow of fluidized material in order to determine the mechanism of formation of distal ramparts commonly seen on SLE deposits [Figure 1]. Our intent is to determine the minimum set of physical processes producing ramparts and to derive basic inferences about emplacement durations, initial velocities, and flow thickness profiles. We use basic volume and momentum conservation equations and explore various source boundary conditions required to reproduce the morphologies of typical SLE craters.

**Geomorphology of Rampart Deposits:** Characteristic features of SLE deposits include: (1) a distal ridge, or "rampart", around the perimeter of the ejecta [Figure 1]; (2) ejecta that appear to have been emplaced as ground-hugging flows originating from close to the crater rim. Measurements on nine SLE craters in Lunae and Solis Plana yield typical crater diameters in the range 3.4–17 km. The ejecta deposits extend ~4–21 km beyond the crater rim. MOLA PEDR profiles across 55 distal ramparts yield heights of 60–80 meters, although the example in Fig. 1(b) is exceptional at 177 m. Rampart widths (0.5–2 km) are narrow with respect to runout distance, which is in marked contrast to distal profiles of large martian and terrestrial landslide deposits [13]. Furthermore, MOLA profiles indicate the ejecta blanket craterward

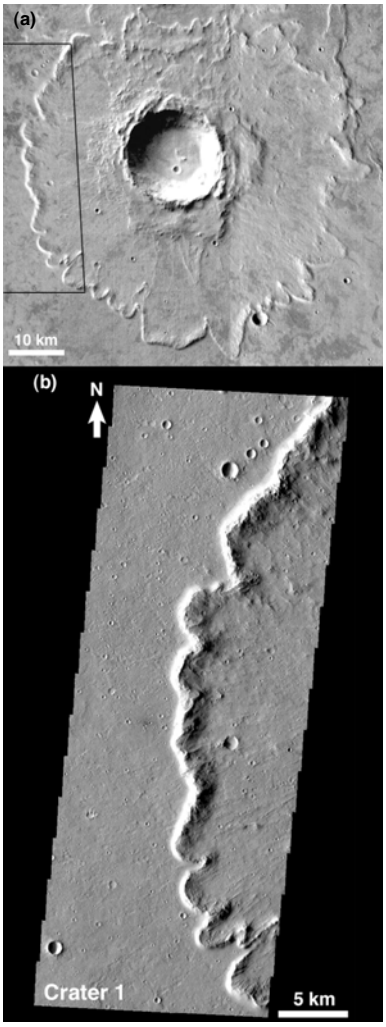


**Figure 1.** SLE crater in Sinai Planitia (21˚S 285˚E) exhibiting well defined distal rampart. (a) THEMIS daytime IR images #I05059003, I06894002 and I08030003. (b) THEMIS visible image V05808002. Outline in (a) shows location of (b).

of the distal rampart has very little relief above the background terrain, implying that much of the ejected material is concentrated in the rampart. In some cases, pre-existing obstacles <100 m divert rather than are surmounted by the flow.

**Ejecta Flow Model:** For emplacement of a continuum surface flow that originates at or close to the crater rim, we can formulate volume and momentum conservation equations in cylindrical coordinates that yield partial differential equations for the flow thickness $h$ and velocity $u$ as a function

of space and time:

$$r\frac{\partial h}{\partial t} + \frac{\partial}{\partial r}(rhu) = 0 \qquad (1),$$

$$\frac{\partial u}{\partial t} + u\frac{\partial u}{\partial r} = -\beta u \qquad (2).$$

The right hand side of eq. (2) describes a local resistance to flow linearly proportional to flow rate, as represented by the constant $\beta$. Values for this parameter can be estimated from $u(r,t)$ by recognizing that the flow has to decelerate to $u$=0 over the radial distance covered by the ejecta deposit.

Solution of eq. (1) for flow depth $h(r,t)$, first requires solution of eq. (2) for $u(r,t)$ as well as specification of source boundary conditions on $h$ and $u$. Equations (3) and (4) show source conditions which, taken together, represent an initial rapid waxing of the flow volume at the source, followed by a more gradual waning phase, as would be expected for the rapid onset of an ejecta flow.

$$h(r_o,t) = h_{\max}\frac{t}{\Gamma_h}e^{1-\frac{t}{\Gamma_h}} \qquad (3)$$

$$u(r_o,t) = \frac{u_o}{1+t/\Gamma_u} \qquad (4).$$

Here $h_{max}$ indicates the maximum flow thickness at the source ($r$=$r_o$), and $u_o$ the initial source velocity. The constants $\Gamma_h$ and $\Gamma_u$ control the rate of decay of the subscripted variables. Having completely specified the problem, solution of eqs. (1) and (2) can proceed by the method of characteristics.

**Application to Observed Craters:** Exploration of the model inputs $h_{max}$, $u_o$, $\beta$, $\Gamma_h$ and $\Gamma_u$ allows us to find the parameter sets that reproduce the observed features of our crater examples. Figure 2 shows flow thickness profiles (normalized to $h_{max}$) at various times for an ejecta flow traveling from the crater rim at $r_o$=4 km to a maximum extent at $r$=14 km. It is clear that as the flow decelerates due to the resistance term in eq. (2), the flow front steepens to produce a distal peak.

**Discussion:** What becomes clear from further exploration of the model parameters is that a radially narrow distal rampart exists only for a very narrow range of inputs. When the velocity decay constant $\Gamma_u$ becomes comparable to the duration of emplacement a broad medial profile is formed. No matter how long the time is continued, a sharp distal margin is never formed. To produce a sharp distal rampart, the ratio of the duration of emplacement to $\Gamma_u$ must be small, i.e., the decay of the velocity at the origin of the flow is very small. Thus, our preliminary finding is that a

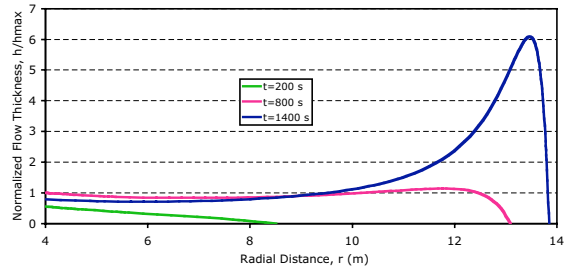


**Figure 2.** Profiles of flow thickness as a function of radial distance for three different times. As the flow decelerates a sharp distal rampart is formed. Parameters for this simulation: $h_{max}$=20 m, $u_o$=30 m s$^{-1}$, $\beta$=0.003, $\Gamma_h$=750 s, $\Gamma_u$=10$^4$ s, crater radius $r_o$=4 km, maximum ejecta extent =10 km from crater rim. The corresponding emplacement duration is ~25 minutes.

rapidly decaying velocity boundary condition does not produce the distal ramparts.

Furthermore, we find that the local resistance to flow is another key factor in producing ramparts in the flow deposit. With the appropriately specified velocity boundary condition and the $-\beta u$ term in eq. (2), the momentum equation then naturally produces flow thickness profiles with sharp distal peaks.

Finally, we note that only modest values of the initial velocity (20–40 m s$^{-1}$) and maximum source flow thickness (10–30 m) are required to produce distal peaks of the order of measured rampart heights. This is consistent with observations in numerous locations that obstacles <100 m high are not overtopped by the ejecta. Given the prodigious energies of the impact process, the mechanism for retarding the continuum flow boundary conditions has yet to be determined. Candidate processes for reconciling our theoretical results and morphologic observations with crater excavation models include atmospheric 'backflow' circulation effects [9,13] or possibly effects due to pre-existing layering in the target substrate. The fact remains that airless bodies with no evidence of volatile stratification (Moon, Mercury) do not produce rampart craters.

**References:** [1] Barlow N. G. et al. (2000) *JGR,105,* 26,733-26,738. [2] Mouginis-Mark P. J. and Boyce J. M. (2005) *Icarus*, submitted. [3] Carr M. H. et al. (1977) *JGR, 82*, 4055-4065. [4] Gault D. E. and Greeley R. (1978) *Icarus, 34,* 486-495. [5] Mouginis-Mark P. J. (1978) *Nature, 272*, 691-694. [6] Mouginis-Mark P. J. (1981) *Icarus, 45,* 60-76. [7] Mouginis-Mark P. J. (1987) *Icarus, 71,* 268-286. [8] Schultz P. H. and Gault D. E. (1979) *JGR, 84,* 7669-7687. [9] Barnouin-Jha O. S. and Schultz P. H. (1998) *JGR*, *103*, 25,739-25,756. [10] Mouginis-Mark P. J. (1979) *JGR, 84,* 8011-8022. [11] Horner V. M. and Greeley R. (1987) *Proc. 17th LPSC, JGR, 92,* E561-E569. [12] Barlow N. G. and Perez C. B. (2003) *JGR, 108,* doi:10.1029/2002JE002036. [13] Barnoiun-Jha O. S. et al. (2004) *JGR,* in press.